ChemPubSoc Europe
DOI: 10.1002/cmdc.201700787
Full Papers

Design, Synthesis, and Biological Evaluation of Bivalent Ligands Targeting Dopamine D_2-Like Receptors and the μ-Opioid Receptor

Mingcheng Qian,[a, b] Lakshmi Vasudevan,[b] Jelle Huysentruyt,[b] Martijn D. P. Risseeuw,[a] Christophe Stove,[b] Patrick M. L. Vanderheyden,[c] Kathleen Van Craenenbroeck,[b] and Serge Van Calenbergh*[a]

Currently, there is mounting evidence that intermolecular receptor–receptor interactions may result in altered receptor recognition, pharmacology and signaling. Heterobivalent ligands have been proven useful as molecular probes for confirming and targeting heteromeric receptors. This report describes the design and synthesis of novel heterobivalent ligands for dopamine D_2-like receptors (D_2-likeR) and the μ-opioid receptor (μOR) and their evaluation using ligand binding and functional assays. Interestingly, we identified a potent bivalent ligand that contains a short 18-atom linker and combines good potency with high efficacy both in β-arrestin 2 recruitment for μOR and MAPK-P for D_4R. Furthermore, this compound was characterized by a biphasic competition binding curve for the D_4R–μOR heterodimer, indicative of a bivalent binding mode. As this compound possibly bridges the D_4R–μOR heterodimer, it could be used as a pharmacological tool to further investigate the interactions of D_4R and μOR.

Introduction

G protein-coupled receptors (GPCRs) represent the largest family of membrane proteins. About half of the clinically used drugs today recognize GPCRs. It is now widely accepted that different GPCRs can interact with each other and form complexes, so-called heteromers. The first hypothesis on GPCR heteromers was raised in the early 1980s after observations of neuropeptide-monoamine receptor–receptor interactions.[1,2] The existence of heteromers was confirmed almost twenty years later for two nonfunctional GPCR monomers, γ-amino butyric acid (GABA) receptors, GABAB1 and GABAB2, which assemble at the cell surface in a signaling heterodimer, the GABAB receptor.[3] Dimerization has now been described for many GPCRs in in vitro settings, although evidence in native tissue is still sparse.[4,5]

In classical pharmacology, allosteric mechanisms were only discussed in terms of intramolecular interactions within a receptor between orthosteric and allosteric sites. Nowadays, there is mounting evidence that intermolecular receptor–receptor interactions may also result in altered receptor recognition, pharmacology and signaling. Heterobivalent ligands have been proven useful as molecular probes for confirming and targeting heteromeric receptors,[6–8] such as κ- and δ-opioid receptor heteromers.[7]

There are five dopamine receptor subtypes that can be divided into two distinct subfamilies: D_1-like (D_1R and D_5R) and D_2-like (D_2R, D_3R, and D_4R). In this study we focus on the heterodimerization of the dopamine D_2-like receptors (D_2-likeR) and the μ-opioid receptor (μOR). D_2-likeR and μOR are GPCRs, expressed in the brain, which play a major role in schizophrenia, Parkinson's disease, addiction, and pain. Heterobivalent ligands are valuable tools to demonstrate the presence of receptor heteromers even in native tissue and can be used to study a specific GPCR dimer behavior without any receptor modification.[9–11] Such compounds may also eventually evolve to useful pharmacological agents.[10] Heterobivalent ligands with a spacer of optimal length are envisaged to exhibit potency greater than that derived from the two monovalent pharmacophores and may allow the targeting of certain heteromeric subtypes, increasing the selectivity of drug action.[11–13]

The dopaminergic and opioid peptide system are pharmacological targets for the treatment of addiction and chronic pain. They show an impressive co-distribution in many nuclei of the brain, which enables intermolecular receptor–receptor interactions[14,15] that may be relevant for the treatment of addiction and chronic pain. In vivo studies indicate the presence of cross-regulation between the D_2-likeR and the μOR. Activation

[a] M. Qian, Dr. M. D. P. Risseeuw, Prof. S. Van Calenbergh
Laboratory for Medicinal Chemistry, Ghent University, Ottergemsesteenweg 460, 9000 Ghent (Belgium)
E-mail: Serge.VanCalenbergh@UGent.be
[b] M. Qian, L. Vasudevan, J. Huysentruyt, Prof. C. Stove, Prof. K. Van Craenenbroeck
Laboratory of Toxicology, Ghent University, Ottergemsesteenweg 460, 9000 Ghent (Belgium)
[c] Prof. P. M. L. Vanderheyden
Department Research Group of Molecular and Biochemical Pharmacology, Faculty of Sciences and Bioengineering Sciences, Vrije Universiteit Brussel, VUB-MBFA, Pleinlaan 2, 1050 Brussels (Belgium)
Supporting information and the ORCID identification number(s) for the author(s) of this article can be found under: https://doi.org/10.1002/cmdc.201700787.

of dopaminergic receptors causes a transient decrease in μOR immunoreactivity. Additionally, D_2-likeR/μOR interactions modulate morphine-induced upregulation of certain transcription factors such as c-Fos, δFosB, and P-CREB.[16–19] These results can be explained by the presence of direct D_2-likeR–μOR interactions. Furthermore, we have identified heterodimerization of D_2R–μOR and D_4R–μOR by co-immunoprecipitation (co-IP) and bioluminescence resonance energy transfer (BRET) studies in mammalian transfected cells (unpublished results). Therefore, all results discussed above indicate that D_2-likeR (especially D_2R and D_4R) and μOR heterodimers could be therapeutic targets for the treatment of addiction and chronic pain.

Herein we report the design and synthesis of a series of heterobivalent μOR agonist/antagonist–D_2-likeR agonist/antagonist ligands as pharmacological tools to further study μOR–D_2-likeR (μOR–D_2R and μOR–D_4R) heteromers. In these compounds, the D_2-likeR agonist/antagonist and the μOR agonist/antagonist were linked through a spacer of variable length. The spacers were based on polyethylene glycol (PEG) unit repeats, and their size was varied (from 18 to 24 atoms) to probe the best interaction with μOR–D_2-likeR heteromers. The binding properties of these compounds were determined by radioligand binding studies in membrane preparations and intact cells. Furthermore, mitogen-activated protein kinase (MAPK) phosphorylation and β-arrestin 2 recruitment assays were performed to test the pharmacological response of the ligands for D_2-likeR and μOR, respectively. Experiments to evaluate the binding of the heterobivalent ligands to μOR and D_2-likeR were performed in cells expressing both μOR and D_2-likeR.

Design of heterobivalent ligands based on the structure of D_2-likeR ligands and μOR ligands

As depicted in Figure 1, the bivalent ligands were derived from the μOR-specific agonist hydromorphone (HM) and the structurally related μOR antagonist naltrexone (NTX). As D_2-likeR ligands we used the antagonist 1,4-disubstituted aromatic piperazines (DAPs, **3**)[20] and the agonist 5-hydroxy-2-(dipropylamino)tetralin (DPAT, **7**)[11] that were equipped with an appropriate ligation handle.

The dimeric ligands were constructed around PEG spacers of variable length that were equipped with a carboxylic acid on one and an azide on the other end (Figure 2). The use of PEG linkers precludes cumulative incremental increases in hydrophobicity that would occur upon homologation if an alkyl chain were used. With the use of existing procedures both opioid ligands **1a** and **1b** were converted into their corresponding 6′-*R*-amino derivatives **2a** and **2b**. The introduced

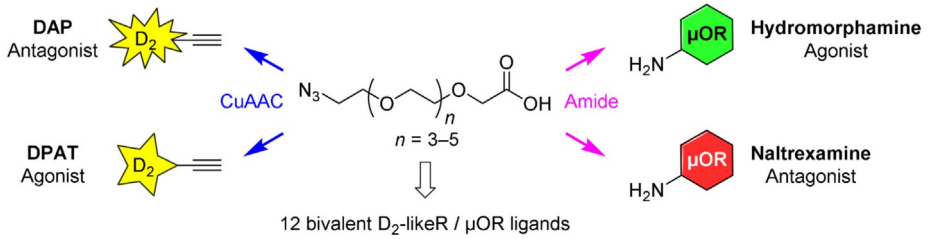

Figure 1. Designed heterobivalent ligands.

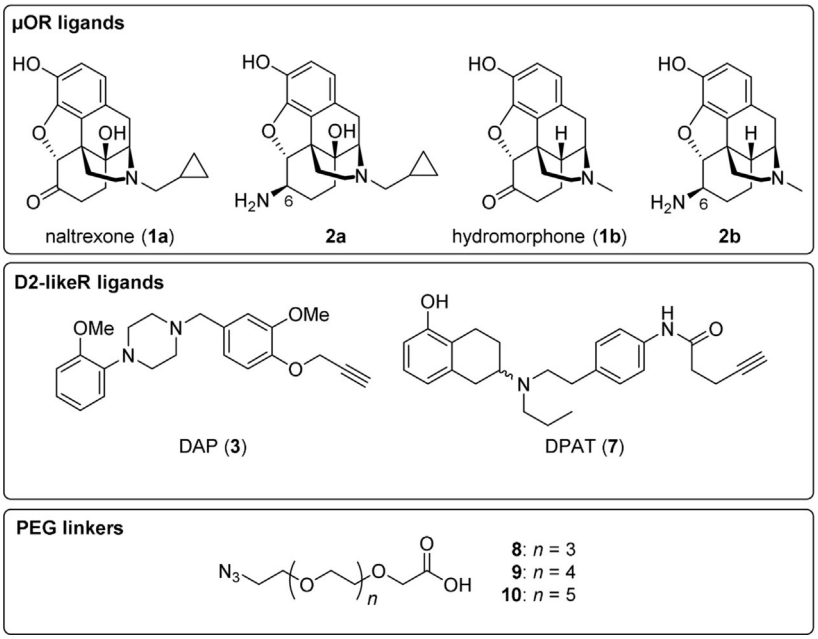

Figure 2. Overview of used monovalent ligands and spacer molecules with appropriate ligation handles.

amine groups allow coupling to the PEG spacers via an amide bond, whereas the azido group on the PEG linker allows facile connection to the alkyne derived dopamine ligands via a copper-catalyzed azide–alkyne cycloaddition (CuAAC) reaction. The choice of the position and nature of the attachment points for linking the two pharmacophore units to the spacer relies on two criteria: the feasibility of the chemical modification and the compatibility of the modification with the biological activity (SAR data) of the pharmacophore.

As indicated above, the selected D_2-likeR ligands need to be functionalized with an alkyne moiety to allow conjugation to the azide group of the PEG linkers. The intrinsic activity of DAPs for D_2-likeR is determined by an aromatic headgroup and an amine moiety, which forms a strong hydrogen bond to the crucial Asp3.32 residue in the transmembrane helix 3 (TM3) of D_2R.[20] A lipophilic appendage is necessary for enhancing ligand affinity. Because proper elongation of this appendage is expected to lead to the "entrance region" of the receptor and from there to the binding pocket of a neighboring protomer, the *para* position of an aromatic moiety terminating this appendage is considered an appropriate point of attachment for a linker unit.[20] Vanillin allows facile introduction of an alkyne group in the *para* position, while reductive amination permits coupling to the phenylpiperazine moiety.

DPAT is a prototypical D_2R/D_3R agonist suitable for constructing bivalent ligands.[21] Site-directed mutagenesis has demonstrated that the 2-aminotetralin moiety interacts with an agonist binding domain involving TM3 and TM5 for activation of either D_2R or D_3R. The basic nitrogen atom and the 5-hydroxy group are critically important for binding affinity. A known aniline derivative of DPAT[11] was coupled with 4-pentynoic acid to afford compound **7** with an alkyne group for CuAAC reaction.

Results and Discussion

Chemistry

Individual components of the bivalent ligands

As μOR ligands the known *R*-amines **2a** and **2b** were prepared from NTX (**1a**) and HM (**1b**), respectively, according to published procedures.[22] Briefly, compounds **1a** and **1b** were converted into the corresponding oximes, which were reduced to 6*R*-amines **2a** and **2b** in the presence of $ZrCl_4$ and $NaBH_4$. Although previous studies showed little stereoselectivity in opioid binding for 6*R* versus 6*S* amine diastereomers,[23] the predominant *R* diastereomers were separated from their *S* epimers by silica gel chromatography, to facilitate further characterization.

For the synthesis of the first alkyne-functionalized D_2-likeR ligand, DPAT (**7**), commercially available 5-methoxyl-2-tetralone (**4**) was converted into the 1,2,3,4-tetrahydronaphthalen-2-amine derivative **5** in four steps following published procedures.[11] Arylamine **5** was coupled with 4-pentynoic acid to give amide **6**. Deprotection of the methyl ether with Me_2SBF_3 in CH_2Cl_2 gave the desired compound **7** (Scheme 1). The alkyne-functionalized D_2-likeR ligand DAP (**3**) was synthesized by starting from vanillin as described earlier by Kühhorn et al.[20] The bifunctional PEG linkers were prepared as described earlier.[24–26]

Bivalent ligand synthesis

The bivalent ligands were generated by first condensing each of the two μOR ligands with each of the three PEG linkers in the presence of the coupling agent EDC and triethylamine to yield the six intermediate azides **11a–f** (Scheme 2). The series

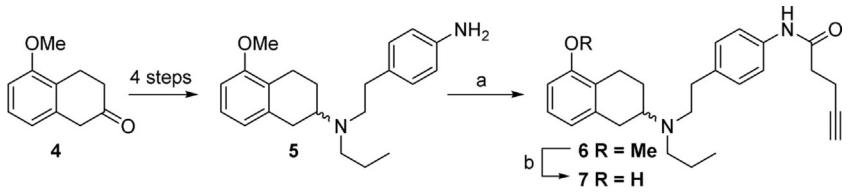

Scheme 1. Reagents and conditions: a) 4-pentynoic acid, (3-dimethylaminopropyl)-*N*-ethylcarbodiimide hydrochloride, triethylamine, CH_2Cl_2, RT, overnight; b) Me_2SBF_3, CH_2Cl_2, RT, overnight.

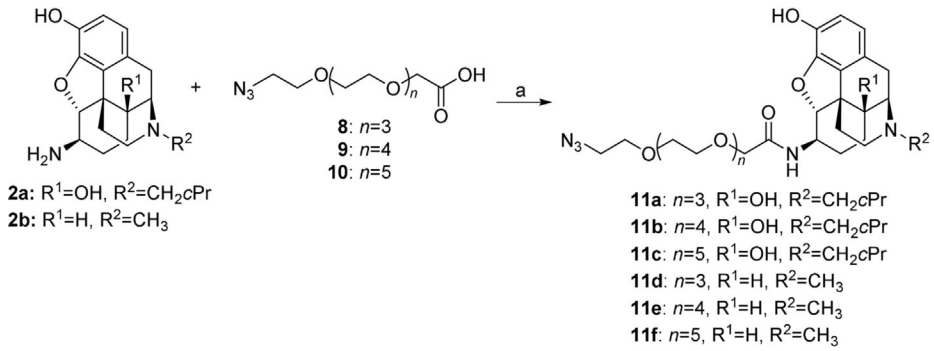

Scheme 2. Reagents and conditions: a) (3-dimethylaminopropyl)-*N*-ethylcarbodiimide hydrochloride, 1-hydroxybenzotriazole, triethylamine, CH_2Cl_2.

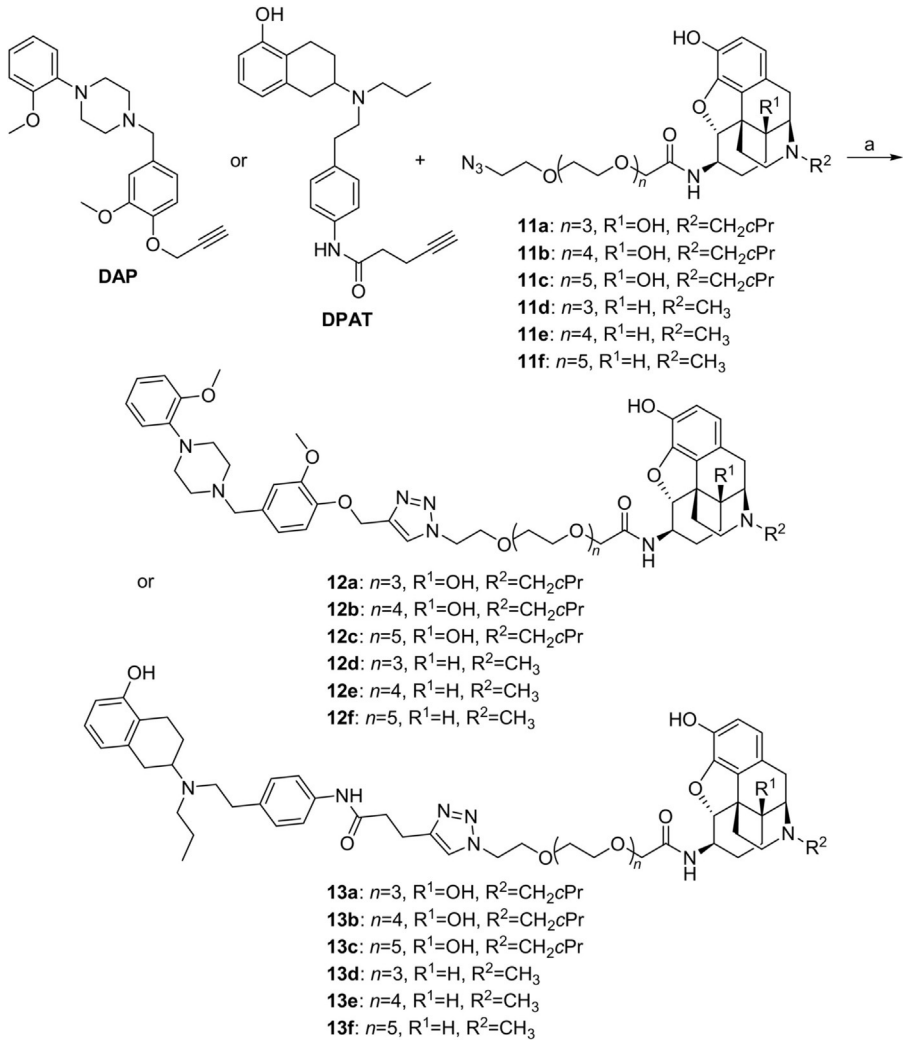

Scheme 3. Reagents and conditions: a) sodium ascorbate, $CuSO_4$, triethylamine, tris[(1-benzyl-1,2,3-triazol-4-yl)methyl]amine, dimethylformamide.

of bivalent ligands was finalized by conjugating each of the six azides to both DPAT and DAP through CuAAC (Scheme 3). This yielded a concise series of 12 bivalent D_2-likeR–μOR ligands in which each of the sets of ligands and the three linkers are systematically represented.

Ligand binding assays

Evaluating the binding of bivalent ligands to the D_2-likeR

A saturation binding assay for [^{3}H]spiperone, a nonselective antagonist of D_2-likeR, was described previously.[27,28] Here we performed a competition assay to evaluate the binding of the bivalent ligands to the D_2-likeR D_2R and D_4R. First the binding affinity of the bivalent ligands **12a–f** and **13a–f** along with their alkynylated DAP and DPAT precursors **3** and **7** was measured by displacement of [^{3}H]spiperone from the D_4R expressed in HEK293T cells, indicating that all the bivalent ligands bind to the D_4R (Table 1). However, a clear decrease in the D_4R binding affinities of the bivalent ligands was detected relative to the alkynes **3** and **7**. Compound **12d** with a short spacer

Table 1. Binding affinities for D_4R and D_4R–μOR.

Compd	R^1	R^2	n	K_i [nM][a]	
				D_4R	D_4R–μOR
3	–	–	–	1.6 ± 0.2	2.1 ± 0.3
12a	OH	CH_2cPr	3	117 ± 12	nd[b]
12b	OH	CH_2cPr	4	214 ± 11	219 ± 10
12c	OH	CH_2cPr	5	226 ± 18	nd
12d	H	CH_3	3	184 ± 35	–
12e	H	CH_3	4	369 ± 42	368 ± 10
12f	H	CH_3	5	339 ± 50	417 ± 8.8
7	–	–	–	15 ± 6.1	16 ± 2.5
13a	OH	CH_2cPr	3	118 ± 12	101 ± 1.3
13b	OH	CH_2cPr	4	157 ± 30	nd
13c	OH	CH_2cPr	5	138 ± 25	nd
13d	H	CH_3	3	110 ± 9.3	nd
13e	H	CH_3	4	191 ± 9.5	394 ± 12
13f	H	CH_3	5	199 ± 16	493 ± 11

[a] Binding affinities were obtained by competitive displacement of radiolabeled [^{3}H]spiperone binding to HEK293T D_4R and HEK293T D_4R–μOR membranes. All values are the mean ± SEM of three independent assays using 11 different ligand concentrations, each performed in duplicate. [b] Not determined.

length (18 atoms) showed a slightly higher affinity for D_4R than **12e** and **12f**. This trend was also apparent for the other bivalent ligands (**12a**, **13a** and **13d**) possessing the same spacer as **12d**. In a next step we wanted to compare the affinity of the bivalent ligands for D_4R in the absence and presence of overexpressed μOR. Unexpectedly, no major differences in K_i values were found between both experimental setups, except for **12d**. Interestingly, a biphasic competition curve was observed for **12d** from which two individual affinity constants could be derived ($K_{i\,high}$ 1.2 ± 0.3 nM and $K_{i\,low}$ 207 ± 51 nM, Figure 3a). Such biphasic competition binding curves are indicative of a bivalent binding mode.[11] Specifically, the high-affinity K_i value represents a bivalent receptor-bridging binding mode of **12d** to D_4R/μOR heterodimer, whereas the low-affinity K_i value reveals a monovalent binding mode to D_4R. Bivalent ligand **12d** thus displays a 170-fold preference for the high-affinity bivalent interaction with the D_4R/μOR heterodimer over monovalent binding mode to D_4R.

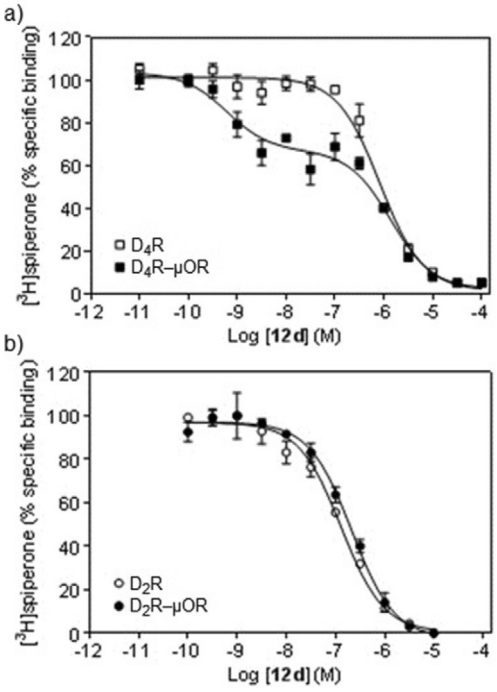

Figure 3. Representative competition curves for bivalent ligand **12d**. D_2-likeR binding of the bivalent ligand **12d** was measured by displacement of the radiolabeled [^{3}H]spiperone from membranes of HEK293T cells co-expressing D_4R/μOR (or D_2R/μOR) or mono-expressing D_4R (or D_2R) only. a) D_4R binding of **12d** in the presence (■, $K_{i\,high}$ 1.2 ± 0.3 nM, $K_{i\,low}$ 207 ± 51 nM) or absence (□, K_i 184 ± 35 nM) of μOR. b) D_2R binding of **12d** in the presence (●, K_i 101 ± 10 nM) or absence (○, K_i 62 ± 3 nM) of μOR. Data are the mean ± SEM of three independent assays, each performed in duplicate.

By following the same approach and still using [^{3}H]spiperone as the radioligand, we also tested the affinity of the bivalent ligand **12d** and its corresponding monovalent ligand **3** to the D_2R and D_2R–μOR receptors. The affinities of compound **12d** to D_2R and D_2R–μOR decreased three-fold relative to the ligand **3** for both receptors (Table 2). Unfortunately, we only obtained a monophasic competition binding curve for **12d** to D_2R–μOR, and no major differences in binding affinity were observed between cells expressing only D_2R and cells expressing both D_2R and μOR (Figure 3b).

Table 2. Binding affinities for D_2R and D_2R–μOR.

Compd	K_i [nM][a]	
	D_2R	D_2R–μOR
3	22 ± 5	32 ± 11
12d	62 ± 3	101 ± 10

[a] Binding affinities were obtained by competitive displacement of radiolabeled [^{3}H]spiperone binding to HEK293T D_2R and HEK293T D_2R–μOR membranes. All values are the mean ± SEM of at least two independent assays.

Next, following a similar protocol, we determined the affinity of monomeric ligand **3** and bivalent ligand **12d** on cells expressing D_2R and D_2R–μOR, using an alternative radioligand, [^{3}H]raclopride. Raclopride, which acts as a selective D_2R antagonist, is more hydrophilic and has substantially less nonspecific binding in intact cells than spiperone. Furthermore, it is not cell permeable, rendering the assay possibly more sensitive, as binding of the radioligand to be displaced is restricted to receptors in the plasma membrane. In this experiment (Table 3) the affinities of **12d** to D_2R and D_2R–μOR were 32.4 ± 8.5 nM and 38.6 ± 3.2 nM, respectively, while the affinities of the monovalent alkyne **3** were 43.1 ± 9.0 nM and 49.9 ± 5.8 nM, respectively. Still, only one-site binding curves for **12d** were obtained from cells mono-expressing D_2R and cells co-expressing D_2R and μOR (Supporting Information). The saturation binding data for [^{3}H]raclopride can be found in the Supporting Information. Interestingly, we found that the affinity of **12d** for D_4R decreased 100-fold relative to the monovalent ligand **3**, while its K_i value for D_2R only decreased three-fold.

Table 3. Binding affinities (K_i) for D_2R and D_2R–μOR.

Compd	K_i [nM][a]	
	D_2R	D_2R–μOR
3	43.1 ± 9.0	49.9 ± 5.8
12d	32.4 ± 8.5	38.6 ± 3.2

[a] Binding affinities were obtained by competitive displacement of radiolabeled [^{3}H]raclopride binding to HEK293T D_2R and HEK293T D_2R–μOR intact cells. All values are the mean ± SEM of at least two independent experiments.

Evaluating the binding of the bivalent ligands to μOR

We performed competitive receptor binding assays in cell membranes expressing μOR to determine the binding affinity of bivalent ligands, using the tracer [^{3}H]diprenorphine, which is a nonselective opioid antagonist. Saturation binding assays showed that the K_d value and B_{max} of [^{3}H]diprenorphine were 0.21 ± 0.064 nM and 489 ± 28 fmol mg^{-1} for μOR, respectively. In the competition assay the binding affinities for the monova-

lent ligands HM and NTX were 4.4±0.21 nM and 7.8±0.16 nM, respectively (Table 4). Compounds **12a–c** and **13a–c**, which were derived from NTX, exhibited a binding affinity for μOR similar to that of NTX, whereas bivalent ligands **12b** and **13b**, with a 21-atom spacer, displayed relatively lower K_i values than the other NTX-based ligands. HM-based bivalent ligands **12d–f** and **13d–f** showed a small decrease in the binding affinities for μOR relative to the corresponding monovalent compound HM, except for **12e** (3.7±0.02 nM) and **13e** (7.2±0.53 nM) with a medium spacer length (21 atoms). Therefore, the affinities of bivalent ligands with a medium-length spacer (21 atoms) to μOR were relatively higher than the other ligands with shorter (18 atoms) or longer linkers (24 atoms).

Table 4. Binding affinities for μOR.

Compd	R^1	R^2	*n*	K_i [nM][a]
HM	H	CH_3	–	4.4±0.21
NTX	OH	CH_2cPr	–	7.8±0.16
12a	OH	CH_2cPr	3	6.3±1.1
12b	OH	CH_2cPr	4	4.6±0.25
12c	OH	CH_2cPr	5	9.2±0.41
13a	OH	CH_2cPr	3	7.5±0.95
13b	OH	CH_2cPr	4	3.8±0.84
13c	OH	CH_2cPr	5	7.6±0.39
12d	H	CH_3	3	16±0.87
12e	H	CH_3	4	3.7±0.02
12f	H	CH_3	5	11±0.57
13d	H	CH_3	3	13±1.2
13e	H	CH_3	4	7.2±0.53
13f	H	CH_3	5	17±3.4

[a] Binding affinities were obtained by competitive displacement of radiolabeled [^{3}H]diprenorphine binding to HEK293T μOR. All values are the mean±SEM of three independent assays.

Functional assays

MAPK phosphorylation to study D_2-likeR activation by the newly developed bivalent ligands

The mitogen-activated protein kinase (MAPK) phosphorylation assay was used to define the functional activity of the bivalent ligands. The MAPK pathway, also known as the extracellular-signal-regulated kinase (ERK) pathway, consists of an intracellular chain of proteins that transfer the signal from the cell surface receptor to the nuclear DNA or other subcellular targets causing cellular responses. Signaling molecules in this pathway communicate with each other by adding a phosphate group to the neighboring protein. This phosphorylation event functions as an on/off switch, leading to the activation or inhibition of the next signaling molecule in the chain.[29] The most commonly studied element of the MAPK pathway, initiated by GPCR activation, is the phosphorylation of p44/42 MAPK (ERK1/2).

To assess functional activation of the D_2R and D_4R by the above described bivalent ligands, we used a HEK293 cell line stably expressing the D_2R and D_4R, respectively.[30] Unexpectedly, the signal band of MAPK-P for D_2R was quite weak (see Supporting Information). Nevertheless, we found a strong immunoreactive band (Figure 4) for MAPK-P upon activation of D_4R with the agonist dopamine (DA), and with the alkynylated DAP (**3**) and DPAT (**7**). Next, all bivalent ligands were tested in this cell system (Figure 5 and Table 5). We can conclude that all bivalent ligands activate the MAPK signaling pathway. Interestingly, compound **12d** with an 18-atom linker (shown in Table 5) displayed modestly high potency (EC_{50}=0.12±0.04 μM) and relatively high efficacy (92±1%) as compared with the monovalent ligand **3** (EC_{50}=0.21±0.12 μM, E_{max}=75±2%), while the potency of compounds **12a–c** decreased 8- to 16-fold relative to **3**. In addition, all the DAP-bond ligands, except for **12d**, showed similar efficacy (E_{max}=72–85%)

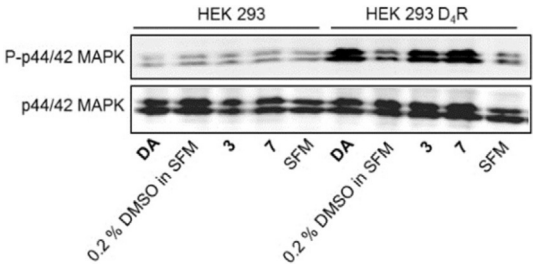

Figure 4. Stimulation of MAPK phosphorylation upon D_4R agonist treatment, as determined by immunoblotting assays. Cells were treated with serum-free media (SFM) for 12 h. Next, D_2-likeR agonists (10 μM), SFM or vehicle control were added for 5 min. Cells were washed and lysed as explained in the Experimental Section. Phosphorylated MAPK was detected by immunoblotting using rabbit anti-phospho-p44/42 MAPK antibody, and mouse anti-p44/42 MAPK antibody was used for demonstrating equal protein loading. The results are representative of three independent experiments; DA=dopamine.

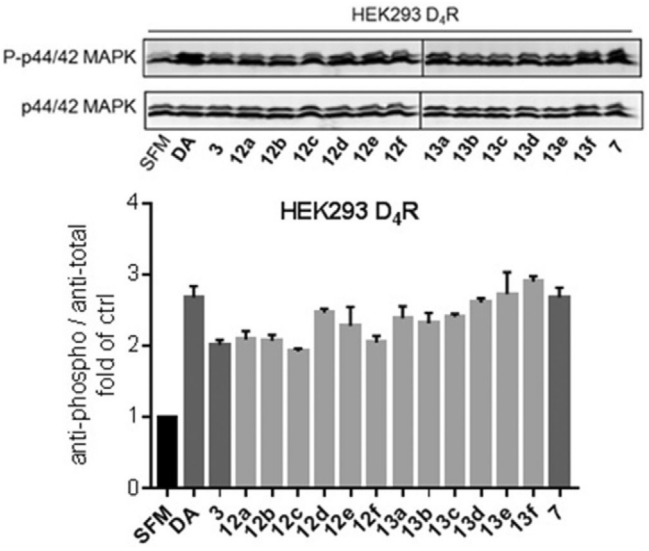

Figure 5. Efficacy of bivalent ligands to phosphorylate MAPK in HEK293 D_4R cells. Cells were treated with serum-free media (SFM) for 12 h. Next, D_2-likeR agonists (10 μM) and SFM were added for 5 min. Cells were washed and lysed as explained in the Experimental Section. Phosphorylated MAPK was detected by immunoblotting using rabbit anti-phospho-p44/42 MAPK antibody, and mouse anti-p44/42 MAPK antibody was used for demonstrating equal protein loading. The top panel shows a representative result from three independent experiments; the bottom panel is given as mean±SEM; DA=dopamine.

Table 5. Potency of D_2-likeR agonists induced MAPK-P in HEK293 D_4R cells.

Compd	R^1	R^2	*n*	EC_{50} [μM][a]	E_{max} [%][b]
DA	–	–	–	0.037 ± 0.012	100 ± 4
3	–	–	–	0.21 ± 0.12	75 ± 2
12a	OH	CH_2cPr	3	3.4 ± 0.2	78 ± 3
12b	OH	CH_2cPr	4	1.9 ± 0.3	77 ± 2
12c	OH	CH_2cPr	5	1.6 ± 0.1	72 ± 1
12d	H	CH_3	3	0.12 ± 0.04	92 ± 1
12e	H	CH_3	4	0.31 ± 0.02	85 ± 5
12f	H	CH_3	5	0.80 ± 0.06	76 ± 2
7	–	–	–	0.37 ± 0.17	100 ± 3
13a	OH	CH_2cPr	3	0.55 ± 0.24	89 ± 4
13b	OH	CH_2cPr	4	0.48 ± 0.06	86 ± 4
13c	OH	CH_2cPr	5	0.88 ± 0.01	90 ± 1
13d	H	CH_3	3	0.95 ± 0.03	97 ± 1
13e	H	CH_3	4	0.57 ± 0.14	101 ± 6
13f	H	CH_3	5	0.45 ± 0.01	108 ± 2

[a] Data are the mean ± SEM of three independent experiments. [b] E_{max} relative to the effect of the reference agonist dopamine at 10 μM.

as compound **3**. On the other hand, DPAT-based bivalent ligands had potency (EC_{50} = 0.45–0.95 μM) and efficacy (E_{max} = 86–108%) similar to those of **7** (EC_{50} = 0.37 ± 0.17 μM, E_{max} = 100 ± 3%). Overall, bivalent ligand **12d** with a short linker length (18 atoms) was the most potent compound to activate the MAPK phosphorylation of D_4R.

β-Arrestin 2 recruitment to μOR

To assess activation of the μOR, the HEK293 cell line was used to stably express the μOR. Unfortunately, we did not obtain any good results from MAPK-P for μOR (data not shown). We then performed a β-arrestin 2 recruitment assay based on the NanoLuc Binary Technology (NanoBiT).[31] Our research group recently reported the application of this assay for monitoring GPCR activation, via ligand-induced interaction of β-arrestin 2 with CB1 and CB2 cannabinoid receptors.[32] Here, we optimized this assay for ligand induced interaction of β-arrestin 2 with μOR. Agonists of μOR, such as [D-Ala^2,*N*-MePhe^4,Gly-ol]-enkephalin (DAMGO), have previously been shown to induce robust receptor phosphorylation, β-arrestin 2 recruitment, and μOR trafficking.[33,34] On the other hand, morphine is a poor inducer of receptor phosphorylation, β-arrestin 2 recruitment, and internalization of μOR. However, upon overexpression of G protein-coupled receptor kinase (GRK2) in cell culture, morphine gained the capacity to induce μOR phosphorylation, accompanied by the rescue of β-arrestin 2 recruitment.[34,35]

To assess the ligand-induced interaction of β-arrestin 2 with μOR, overexpression of GRK2 in cell culture was performed. Our results show that DAMGO induces robust β-arrestin 2 recruitment even in the absence of GRK2. On the other hand, HM could promote β-arrestin 2 recruitment only when GRK2 was overexpressed in HEK293 cells. Both results are in line with those found in the literature (see Supporting Information Figure 2).

Upon stimulation with a known agonist of μOR, HM, μOR-SmBiT showed a concentration dependent interaction with LgBiT-β-arrestin 2 in the presence of GRK2 (Figure 6). Also, for the bivalent ligands containing the agonistic HM-based monomer, concentration dependence was obtained, and EC_{50} values were determined as a measure of relative potency (Table 6 and Figure 6). Ranging from 12.73 nM to 57.06 nM, all the EC_{50} values of the bivalent ligands were similar to that of the parent HM (EC_{50} = 30.09 nM). Amongst the DAP-based ligands, compound **12d**, having the shortest linker (18 atoms), showed excellent potency (EC_{50} = 12.73 nM) and high efficacy (85 ± 3%). Remarkably, all DPAT-based ligands showed lower efficacies than DAP-bond ligands, with compound **13d** having the same spacer as **12d**, displaying the lowest efficacy (24 ± 1%) amongst the DPAT-based ligands.

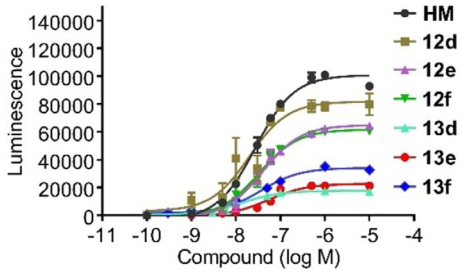

Figure 6. Concentration-dependent interaction of μOR with β-arrestin 2 upon stimulation with agonists of μOR. Data are the mean ± SEM of at least two independent experiments.

Table 6. Potency and maximal effect of μOR agonists on β-arrestin 2 recruitment for μOR.

Compd	R^1	R^2	*n*	EC_{50} [nM] (95% CI)[a]	HM [%][b]
HM	H	CH_3	–	30.09 (24.51–36.94)	100
12d	H	CH_3	3	12.73 (7.612–21.28)	85 ± 3
12e	H	CH_3	4	40.38 (30.41–53.61)	68 ± 1
12f	H	CH_3	5	34.86 (25.76–47.18)	64 ± 1
13d	H	CH_3	3	13.41 (8.286–23.15)	24 ± 1
13e	H	CH_3	4	57.06 (38.49–84.58)	28 ± 1
13f	H	CH_3	5	14.09 (10.14–21.08)	38 ± 1

[a] EC_{50} values are a measure of potency for β-arrestin 2 recruitment. Data are given as EC_{50} values (95% CI profile likelihood). [b] Percent maximal stimulation relative to the agonist HM at 10 μM.

Conclusions

In summary, we have designed and synthesized a series of novel heterobivalent ligands based on the chemical structure of two distinct D_2-likeR ligands and a μOR agonist and antagonist. Ligation of μOR ligands does not perturb the affinity for μOR. μOR bivalent ligands derived from the HM agonist are still capable of activating the μOR signaling pathway as demonstrated by β-arrestin 2 recruitment. Furthermore, bivalent ligand **12d** containing the shortest linker (18 atoms) showed excellent potency and high efficacy both in β-arrestin 2 recruitment for μOR and MAPK-P for D_4R. On the other hand, ligation of D_2-likeR ligands negatively influences the affinity for D_2R

and D_4R when using [^{3}H]spiperone as the radioligand. However, a biphasic competition binding curve was observed for **12 d** to D_4R–μOR, which indicates a bivalent binding mode.[11,36] Hence, compound **12 d** could bridge the D_4R–μOR heterodimer.

Unexpectedly, we were unable to identify bivalent ligands that show a biphasic binding mode or a significant increase in affinity for cells expressing both the D_2R and the μOR, compared with cells that only express D_2R. This indicates that none of the bivalent ligands are capable of binding both receptors simultaneously, possibly owing to a suboptimal length or nature of the selected linkers, which, however, were based on the spacers of class A GPCR bivalent ligands.[20,37] On the other hand, it cannot be excluded that subtle differences such as differences in the dissociation rate of the ligands remain undetected by comparing equilibrium dissociation constants. In a study investigating adenosine A_3 receptors, it was found that ligand binding kinetics is found to be influenced in membrane microdomains as a consequence of receptor dimerization.[38]

While future studies will try to address these shortcomings, the current study already gives access to the monomeric ligands that are equipped with appropriate ligation handles to construct second-generation bivalent ligands with alternative spacers. In conclusion, the present results provide useful insight into development of new bivalent ligands as tools to investigate the μOR-D_4R heterodimer.

Experimental Section

Chemistry

All reactions described were performed under an N_2 atmosphere and at ambient temperature unless stated otherwise. All regents and solvents were purchased from Sigma–Aldrich (Diegem, Belgium), Fisher Scientific (Merelbeke, Belgium), TCI Europe (Zwijndrecht, Belgium) or Apollo Scientific (Bredbury, Stockport, UK) and used as received. NMR solvents were acquired from Eurisotop (Saint-Aubin, France). Reactions were monitored by TLC analysis using TLC aluminum sheets (Macherey–Nagel, Alugram Sil G/UV254) with detection by spraying with a solution of $(NH_4)_6Mo_7O_{24}{\cdot}4H_2O$ (25 g L^{-1}) and $(NH_4)_4Ce(SO_4)_4{\cdot}2H_2O$ (10 g L^{-1}) in H_2SO_4 (10% aq) followed by charring or an aqueous solution of $KMnO_7$ (20 g L^{-1}) and K_2CO_3 (10 g L^{-1}) or an ethanolic solution of ninhydrin (2 g L^{-1}) and acetic acid (1% *v/v*) followed by charring. Solution pH values were estimated using universal indicator paper (Merck). Silica gel column chromatography was performed using a Grace Reveleris X2 system and the corresponding silica gel cartridges. ESI-HRMS spectra were measured with a Waters LCT Premier XE Mass spectrometer calibrated using leucine enkephalin as an external standard. ^{1}H- and ^{13}C-APT-NMR spectra were recorded with a Varian Mercury-300BB (300/75 MHz) spectrometer. Chemical shifts are given in ppm (δ) relative to tetramethylsilane as an internal standard (^{1}H NMR) or the NMR solvent (^{13}C NMR). Coupling constants are given in Hertz (Hz). Weak signals in ^{13}C NMR are indicated as (w). LC–MS analyses were carried out on a Waters AutoPurification System equipped with PDA and ESI-MS detection and using a Waters CORTECS C_{18} column (4.6×100 mm, 2.7 μm) and a water/acetonitrile/formic acid linear gradient system at a flow rate of 1.44 mL min^{-1}.

General procedure 1: Carbodiimide-mediated amide formation

To a solution of (3-dimethylaminopropyl)-*N*-ethylcarbodiimide hydrochloride (1.5 equiv) and 1-hydroxybenzotriazole (1.4 equiv) in CH_2Cl_2 was added a solution of the PEG spacer (1.2 equiv) in CH_2Cl_2 (0.2 M) and cooled to 0 °C under an argon atmosphere. After 15 min at 0 °C, amines **2 a**,**b** (1.0 equiv) were added and triethylamine (2 equiv) was added dropwise; the reaction was slowly warmed to room temperature and stirred overnight. The reaction was diluted with CH_2Cl_2, washed successively with water, HCl (5% aq), $NaHCO_3$ (sat. aq), NaCl (sat. aq), dried over Na_2SO_4, filtered and solvent was evaporated under reduced pressure. The crude product was purified by silica gel chromatography (NH_4OH/MeOH/CH_2Cl_2, 1:5:94 *v/v/v*) to yield the amides **11 a–f**.

General procedure 2: Copper mediated azide-alkyne cycloaddition

To a solution of the intermediate azide (1.0 equiv) in dimethylformamide (0.1 M) was added the alkyne (1.5 equiv), sodium ascorbate (1.0 equiv, 0.5 M), $CuSO_4$ (0.2 equiv, 0.05 M), triethylamine (3.0 equiv) and a catalytic amount of tris[(1-benzyl-1,2,3-triazol-4-yl)methyl]amine. The reaction mixture was stirred overnight at room temperature in the dark under an argon atmosphere. The solvent was evaporated under reduced pressure and the residue was redissolved in water and extracted with CH_2Cl_2. Then combined organic fractions were pooled, washed with brine and dried over Na_2SO_4. The crude compound was purified by silica gel chromatography (NH_4OH/MeOH/CH_2Cl_2, 1:5:94 *v/v/v*) to give the final compound as a white solid (yield, 40–57%).

***N*-(4-(2-((5-methoxy-1,2,3,4-tetrahydronaphthalen-2-yl)(propyl)-amino)ethyl)phenyl)pent-4-ynamide (6)**: To a solution of (3-dimethylaminopropyl)-*N*-ethylcarbodiimide hydrochloride (1.1 g, 4.92 mmol) in CH_2Cl_2 (20 mL) was added a solution of 4-pentynoic acid (0.39 g, 3.93 mmol) in CH_2Cl_2 (5 mL) followed by a solution of **5** (1.1 g, 3.28 mmol) in CH_2Cl_2 (5 mL). The mixture was cooled to 0 °C and triethylamine (0.68 mL, 4.92 mmol) was added dropwise; the reaction was slowly warmed to room temperature and stirred overnight. The reaction was diluted with CH_2Cl_2, washed successively with water, HCl (5% aq), $NaHCO_3$ (sat. aq), NaCl (sat. aq), dried over Na_2SO_4, filtered and solvent was evaporated under reduced pressure. The crude product was purified by silica gel chromatography (hexane/EtOAc, 3:2 *v/v*) to give **6** as a pale-yellow solid (1.32 g, 95%). ^{1}H NMR (300 MHz, $CDCl_3$): δ = 7.42 (d, *J* = 8.4 Hz, 2H), 7.15 (d, *J* = 8.4 Hz, 2H), 7.07 (t, *J* = 7.9 Hz, 1H), 6.69 (d, *J* = 7.8 Hz, 1H), 6.62 (d, *J* = 8.1, 1H), 3.78 (s, 3H), 3.04–2.91 (m, 2H), 2.91–2.80 (m, 1H), 2.79–2.63 (m, 6H), 2.63–2.53 (m, 7H), 2.05 (d, *J* = 3.2 Hz, 2H), 1.61–1.41 (m, 3H), 0.88 ppm (t, *J* = 7.3 Hz, 3H); ^{13}C NMR (75 MHz, $CDCl_3$): δ = 169.4, 157.2, 137.9, 137.0, 135.7, 129.2, 126.1, 125.2, 121.6, 120.1, 106.9, 82.9, 69.5, 56.7, 55.2, 52.9, 52.6, 36.1, 35.4, 32.3, 25.7, 23.8, 22.2, 14.8, 11.9 ppm; HRMS (ESI) *m/z*: calculated for $C_{27}H_{35}N_2O_2$ $[M+H]^+$ 419.2699, found 419.2705.

***N*-(4-(2-((5-hydroxy-1,2,3,4-tetrahydronaphthalen-2-yl)(propyl)-amino)ethyl)phenyl)pent-4-ynamide (7)**: To a solution of **6** (1.05 g, 2.51 mmol) in CH_2Cl_2 (20 mL) was added boron trifluoride methyl sulfide complex (4.77 mL, 45.21 mmol). The reaction was stirred overnight under nitrogen at room temperature. The mixture was treated with a saturated aqueous $NaHCO_3$ solution, extracted with CH_2Cl_2, dried over Na_2SO_4 and the solvent was evaporated under reduced pressure. The crude product was purified by silica gel chromatography (hexane/EtOAc, 1:1 *v/v*) to yield **7** as a white foam (750 mg, 74%). ^{1}H NMR (300 MHz, $CDCl_3$): δ = 7.41 (d, *J* =

8.4 Hz, 2H), 7.14 (d, J=8.4 Hz, 2H), 6.97 (t, J=7.8 Hz, 1H), 6.66 (d, J=7.5 Hz, 1H), 6.59 (d, J=7.8 Hz, 1H), 3.02–2.94 (m, 2H), 2.90–2.82 (m, 1H), 2.79–2.66 (m, 6H), 2.62–2.53 (m, 7H), 2.05 (d, J=3.2 Hz, 2H), 1.66–1.56 (m, 1H), 1.53–1.46 (m, 2H), 0.89 ppm (t, J=7.3 Hz, 3H); ^{13}C NMR (75 MHz, $CDCl_3$): δ=169.1, 153.5, 138.3, 137.1, 135.4, 129.2, 126.3, 123.0, 121.6, 120.0, 111.9, 82.8, 69.7, 56.6, 52.7, 52.6, 36.2, 35.2, 32.2, 25.7, 23.5, 22.0, 14.8, 11.9 ppm; HRMS (ESI) m/z: calculated for $C_{26}H_{33}N_2O_2$ $[M+H]^+$ 405.2542, found 405.2545.

14-azido-*N*-((4*R*,4a*S*,7*R*,7a*R*,12b*S*)-3-(cyclopropylmethyl)-4a,9-dihydroxy-2,3,4,4a,5,6,7,7a-octahydro-1*H*-4,12-methanobenzofuro[3,2-*e*]isoquinolin-7-yl)-3,6,9,12-tetraoxatetradecanamide (11 a): Compound **11 a** was subjected to general procedure 1. Pale-yellow solid, 68%. ^{1}H NMR (300 MHz, $CDCl_3$): δ=6.71 (d, J=8.1 Hz, 1H), 6.56 (dd, J=8.2 Hz, 1H), 4.45 (d, J=7.5 Hz, 1H), 4.01 (s, 2H), 3.74–3.66 (m, 14H), 3.39 (t, J=5.6 Hz, 2H), 3.10–3.04 (m, 2H), 2.99 (s, 1H), 2.67–2.54 (m, 2H), 2.40–2.34 (m, 4H), 2.24–2.13 (m, 2H), 1.89 (dd, J=12.8, 3.1 Hz, 2H), 1.70–1.40 (m, 4H), 0.90–0.77 (m, 1H), 0.57–0.48 ppm (m, 2H); ^{13}C NMR (75 MHz, $CDCl_3$): δ=169.9, 142.4, 140.0, 131.0, 129.0, 128.2, 125.2, 119.1, 117.7, 93.5, 70.9, 70.6, 70.5, 70.5, 70.4, 70.3, 70.0, 62.3, 59.2, 50.7, 50.6, 47.7, 44.0, 30.6, 30.1, 24.4, 22.6, 9.4, 3.9, 3.7 ppm; HRMS (ESI) m/z: calculated for $C_{30}H_{44}N_5O_8$ $[M+H]^+$ 602.3190, found 602.3205.

17-azido-*N*-((4*R*,4a*S*,7*R*,7a*R*,12b*S*)-3-(cyclopropylmethyl)-4a,9-dihydroxy-2,3,4,4a,5,6,7,7a-octahydro-1*H*-4,12-methanobenzofuro[3,2-*e*]isoquinolin-7-yl)-3,6,9,12,15-pentaoxaheptadecanamide (11 b): Compound **11 b** was subjected to general procedure 1. Pale-yellow solid, 62%. ^{1}H NMR (300 MHz, $CDCl_3$): δ=6.70 (d, J=8.1 Hz, 1H), 6.54 (d, J=8.2 Hz, 1H), 4.45 (d, J=7.5 Hz, 1H), 3.99 (s, 2H), 3.73–3.60 (m, 18H), 3.37 (t, J=5.6 Hz, 2H), 3.11 (brs, 1H), 3.01 (d, J=18.4 Hz, 1H), 2.70–2.55 (m, 2H), 2.38 (d, J=6.6 Hz, 2H), 2.26–2.10 (m, 2H), 1.87 (td, J=12.5, 2.9 Hz, 1H), 1.72–1.54 (m, 2H), 1.46 (dt, J=11.3, 2.8 Hz, 2H), 0.91–0.79 (m, 2H), 0.58–0.49 (m, 2H), 0.17–0.09 ppm (m, 2H); ^{13}C NMR (75 MHz, $CDCl_3$): δ=170.0, 142.5, 140.1, 130.9, 124.1, 119.0, 117.8, 93.2, 70.9, 70.6, 70.6, 70.5, 70.5, 70.4, 70.30, 70.0, 70.0, 62.3, 59.1, 50.8, 50.6, 47.6, 44.1, 30.5, 30.1, 24.3, 22.6, 9.3, 3.9, 3.8 ppm; HRMS (ESI) m/z: calculated for $C_{32}H_{48}N_5O_9$ $[M+H]^+$ 646.3452, found 646.3458.

20-azido-*N*-((4*R*,4a*S*,7*R*,7a*R*,12b*S*)-3-(cyclopropylmethyl)-4a,9-dihydroxy-2,3,4,4a,5,6,7,7a-octahydro-1*H*-4,12-methanobenzofuro[3,2-*e*]isoquinolin-7-yl)-3,6,9,12,15,18-hexaoxaicosanamide (11 c): Compound **11 c** was subjected to general procedure 1. Pale-yellow solid, 56%. ^{1}H NMR (300 MHz, $CDCl_3$): δ=6.71 (d, J=8.1 Hz, 1H), 6.56 (d, J=8.1 Hz, 1H), 4.45 (d, J=7.5 Hz, 1H), 4.00 (s, 2H), 3.75–3.60 (m, 22H), 3.38 (t, J=5.1 Hz, 2H), 3.10–2.98 (m, 2H), 2.59 (dd, J=19.1, 6.3 Hz, 2H), 2.36 (d, J=6.5 Hz, 2H), 2.24–2.08 (m, 2H), 1.90 (qd, J=12.7, 3.2 Hz, 1H), 1.72–1.53 (m, 2H), 1.46 (dd, J=9.0, 4.4 Hz, 2H), 0.83 (dp, J=13.0, 6.3 Hz, 2H), 0.56–0.49 (m, 2H), 0.12 ppm (d, J=4.7 Hz, 2H); ^{13}C NMR (75 MHz, $CDCl_3$): δ=169.9, 142.4, 140.0, 131.0, 124.3, 119.0, 117.7, 93.3, 70.9, 70.6, 70.6, 70.6, 70.5, 70.5, 70.4, 70.4, 70.3, 70.0, 70.0, 62.3, 59.2, 50.8, 50.6, 47.7, 44.0, 30.6, 30.1, 24.4, 22.6, 9.4, 3.9, 3.7 ppm; HRMS (ESI) m/z: calculated for $C_{34}H_{52}N_5O_{10}$ $[M+H]^+$ 690.3714, found 690.3744.

14-azido-*N*-((4*R*,4a*R*,7*R*,7a*R*,12b*S*)-9-hydroxy-3-methyl-2,3,4,4a,5,6,7,7a-octahydro-1*H*-4,12-methanobenzofuro[3,2-*e*]isoquinolin-7-yl)-3,6,9,12-tetraoxatetradecanamide (11 d): Compound **11 d** was subjected to general procedure 1. Off-white solid, 62%. ^{1}H NMR (300 MHz, $CDCl_3$): δ=6.66 (d, J=8.1 Hz, 1H), 6.56 (d, J=8.1 Hz, 1H), 4.41 (d, J=7.9 Hz, 1H), 3.96 (s, 2H), 3.72–3.57 (m, 14H), 3.37 (t, J=5.6 Hz, 2H), 3.11 (brs, 1H), 2.98 (d, J=18.4 Hz, 1H), 2.54 (dd, J=11.9, 4.4 Hz, 1H), 2.39 (s, 3H), 2.34–2.14 (m, 2H), 1.92–1.75 (m, 2H), 1.71–1.48 (m, 3H), 1.42–1.23 (m, 2H), 1.14–1.00 ppm (m, 1H); ^{13}C NMR (75 MHz, $CDCl_3$): δ=169.9, 142.8, 140.3, 129.3, 125.2, 119.4, 117.5, 93.2, 70.8, 70.6, 70.5, 70.4, 70.4, 70.4, 70.2, 70.0, 59.4, 51.5, 50.6, 47.2, 44.9, 43.4, 42.6, 35.2, 28.8, 24.1, 20.1 ppm; HRMS (ESI) m/z: calculated for $C_{27}H_{40}N_5O_7$ $[M+H]^+$ 546.2928, found 546.2923.

17-azido-*N*-((4*R*,4a*R*,7*R*,7a*R*,12b*S*)-9-hydroxy-3-methyl-2,3,4,4a,5,6,7,7a-octahydro-1*H*-4,12-methanobenzofuro[3,2-*e*]isoquinolin-7-yl)-3,6,9,12,15-pentaoxaheptadecanamide (11 e): Compound **11 e** was subjected to general procedure 1. Off-white solid, 53%. ^{1}H NMR (300 MHz, $CDCl_3$): δ=6.59 (d, J=8.1 Hz, 1H), 6.51 (d, J=8.1 Hz, 1H), 4.36 (d, J=7.9 Hz, 1H), 3.92 (s, 2H), 3.73–3.54 (m, 18H), 3.34 (t, J=5.6 Hz, 2H), 2.95 (d, J=19.1 Hz, 1H), 2.49 (dd, J=12.5, 4.2 Hz, 1H), 2.39–2.29 (m, 2H), 2.20 (s, 3H), 1.79 (dd, J=12.4, 4.6 Hz, 2H), 1.68–1.55 (m, 2H), 1.33–1.20 (m, 2H), 1.07 ppm (t, J=7.2 Hz, 1H); ^{13}C NMR (75 MHz, $CDCl_3$): δ=169.8, 143.0, 140.7, 129.3, 124.8, 119.2, 117.5, 92.8, 70.8, 70.6, 70.5, 70.4, 70.4, 70.3, 70.3, 70.2, 69.9, 59.3, 51.6, 47, 45.0, 43.4, 42.7 (d, J=5.2 Hz), 38.9, 35.3, 28.9, 24.1, 20.0, 15.49 ppm; HRMS (ESI) m/z: calculated for $C_{29}H_{44}N_5O_8$ $[M+H]^+$ 590.3190, found 590.3192.

20-azido-*N*-((4*R*,4a*R*,7*R*,7a*R*,12b*S*)-9-hydroxy-3-methyl-2,3,4,4a,5,6,7,7a-octahydro-1*H*-4,12-methanobenzofuro[3,2-*e*]isoquinolin-7-yl)-3,6,9,12,15,18-hexaoxaicosanamide (11 f): Compound **11 f** was subjected to general procedure 1. Off-white solid, 51%. ^{1}H NMR (300 MHz, $CDCl_3$): δ=6.64 (d, J=8.1 Hz, 1H), 6.54 (d, J=8.1 Hz, 1H), 4.42 (d, J=8.0 Hz, 1H), 3.95 (s, 2H), 3.76–3.49 (m, 22H), 3.36 (t, J=5.6 Hz, 2H), 3.10 (brs, 1H), 2.93 (s, 2H), 2.86 (d, J=0.6 Hz, 1H), 2.58–2.46 (m, 1H), 2.37 (s, 3H), 2.26–2.10 (m, 2H), 1.85 (dt, J=12.0, 6.0 Hz, 1H), 1.70–1.59 (m, 1H), 1.51 (dd, J=13.4, 3.5 Hz, 1H), 1.45–1.20 (m, 2H), 1.06 ppm (ddd, J=15.3, 10.5, 2.4 Hz, 1H); ^{13}C NMR (75 MHz, $CDCl_3$): δ=169.9, 142.8, 140.3, 129.4, 125.2, 119.3, 117.4, 93.1, 70.8, 70.6, 70.6, 70.5, 70.5, 70.4, 70.4, 70.4, 70.3, 70.2, 69.9, 59.3, 51.7, 50.6, 47.2, 43.4, 42.7, 35.2, 28.7, 24.1, 20.0 ppm; HRMS (ESI) m/z: calculated for $C_{31}H_{48}N_5O_9$ $[M+H]^+$ 634.3452, found 634.3444.

***N*-((4*R*,4a*S*,7*R*,7a*R*,12b*S*)-3-(cyclopropylmethyl)-4a,9-dihydroxy-2,3,4,4a,5,6,7,7a-octahydro-1*H*-4,12-methanobenzofuro[3,2-*e*]isoquinolin-7-yl)-14-(4-((2-methoxy-4-((4-(2-methoxyphenyl)piperazin-1-yl)methyl)phenoxy)methyl)-1*H*-1,2,3-triazol-1-yl)-3,6,9,12-tetraoxatetradecanamide (12 a)**: Compound **12 a** was subjected to general procedure 2. Off-white solid, 55%. LC–HRMS: t_R=5.43 min (10–100% MeCN, 15 min run), 96.49%. ^{1}H NMR (300 MHz, $CDCl_3$): δ=7.85 (s, 1H), 7.20 (d, J=8.7 Hz, 1H), 7.00–6.79 (m, 6H), 6.68 (d, J=8.1 Hz, 1H), 6.53 (d, J=8.1 Hz, 1H), 5.28 (d, J=7.1 Hz, 2H), 4.53 (t, J=5.6 Hz, 2H), 4.42 (d, J=7.5 Hz, 1H), 3.93 (s, 2H), 3.87 (t, J=5.2 Hz, 2H), 3.84 (s, 3H), 3.82 (s, 3H), 3.68–3.56 (m, 14H), 3.53 (s, 2H), 3.09–3.03 (m, 5H), 2.95 (d, J=6.4 Hz, 1H), 2.72–2.53 (m, 6H), 2.35 (d, J=6.5 Hz, 2H), 2.21–2.11 (m, 2H), 1.86 (qd, J=12.6, 3.3 Hz, 1H), 1.74–1.62 (m, 1H), 1.61–1.37 (m, 3H), 0.90–0.75 (m, 1H), 0.55–0.47 (m, 2H), 0.15–0.07 ppm (m, 2H); ^{13}C NMR (75 MHz, $CDCl_3$): δ=169.8, 152.2, 149.4, 146.8, 144.1, 142.5, 141.2, 140.2, 131.1, 130.9, 124.2, 124.08, 122.8, 121.7, 120.9, 119.0, 118.2, 118.0, 113.7, 112.9, 111.1, 92.8, 70.8, 70.5, 70.4, 70.4, 70.3, 70.3, 70.0, 69.4, 63.1, 62.7, 62.3, 59.1, 55.8, 55.3, 53.1, 51.0, 50.3, 50.2, 47.6, 44.0, 30.7, 30.0, 24.4, 22.6, 9.4, 3.9, 3.7 ppm; HRMS (ESI) m/z: calculated for $C_{52}H_{71}N_7O_{11}$ $[M+2H]^{2+}$ 484.7600, found 484.7572.

***N*-((4*R*,4a*S*,7*R*,7a*R*,12b*S*)-3-(cyclopropylmethyl)-4a,9-dihydroxy-2,3,4,4a,5,6,7,7a-octahydro-1*H*-4,12-methanobenzofuro[3,2-*e*]isoquinolin-7-yl)-17-(4-((2-methoxy-4-((4-(2-methoxyphenyl)piperazin-1-yl)methyl)phenoxy)methyl)-1*H*-1,2,3-triazol-1-yl)-3,6,9,12,15-pentaoxaheptadecanamide (12 b)**: Compound **12 b** was subjected to general procedure 2. Off-white solid, 52%. LC–

HRMS: t_R = 5.44 min (10–100% MeCN, 15 min run), 92.62%; HRMS (ESI) *m/z*: calculated for $C_{54}H_{75}N_7O_{12}$ $[M+2H]^{2+}$ 506.7731, found 506.7713.

***N*-((4*R*,4a*S*,7*R*,7a*R*,12b*S*)-3-(cyclopropylmethyl)-4a,9-dihydroxy-2,3,4,4a,5,6,7,7a-octahydro-1*H*-4,12-methanobenzofuro[3,2-*e*]isoquinolin-7-yl)-20-(4-((2-methoxy-4-((4-(2-methoxyphenyl)piperazin-1-yl)methyl)phenoxy)methyl)-1*H*-1,2,3-triazol-1-yl)-3,6,9,12,15,18-hexaoxaicosanamide (12c)**: Compound **12c** was subjected to general procedure 2. Off-white solid, 50%. LC–HRMS: t_R = 5.63 min (10–100% MeCN, 15 min run), 95.23%; HRMS (ESI) *m/z*: calculated for $C_{56}H_{79}N_7O_{13}$ $[M+2H]^{2+}$ 528.7862, found 528.7854.

***N*-((4*R*,4a*R*,7*R*,7a*R*,12b*S*)-9-hydroxy-3-methyl-2,3,4,4a,5,6,7,7a-octahydro-1*H*-4,12-methanobenzofuro[3,2-*e*]isoquinolin-7-yl)-14-(4-((2-methoxy-4-((4-(2-methoxyphenyl)piperazin-1-yl)methyl)phenoxy)methyl)-1*H*-1,2,3-triazol-1-yl)-3,6,9,12-tetraoxatetradecanamide (12d)**: Compound **12d** was subjected to general procedure 2. Off-white solid, 42%. LC–HRMS: t_R = 5.23 min (10–100% MeCN, 15 min run), 96.94%. ^{1}H NMR (300 MHz, $CDCl_3$): δ = 7.85 (s, 1H), 7.11 (d, *J* = 8.2 Hz, 1H), 7.01–6.94 (m, 2H), 6.94–6.88 (m, 2H), 6.83 (ddd, *J* = 8.1, 5.5, 1.7 Hz, 2H), 6.68 (d, *J* = 8.1 Hz, 1H), 6.56 (d, *J* = 8.1 Hz, 1H), 5.28 (d, *J* = 6.7 Hz, 2H), 4.53 (t, *J* = 5.7 Hz, 2H), 4.42 (d, *J* = 8.0 Hz, 1H), 3.91 (d, *J* = 1.4 Hz, 2H), 3.87 (t, *J* = 5.5 Hz, 2H), 3.84 (s, 3H), 3.82 (s, 3H), 3.66–3.51 (m, 14H), 3.09 (br s, 4H), 2.98–2.85 (m, 1H), 2.66 (br s, 3H), 2.52 (dd, *J* = 12.1, 4.6 Hz, 1H), 2.39 (s, 3H), 2.19 (dt, *J* = 9.8, 5.3 Hz, 2H), 1.82 (td, *J* = 12.2, 5.1 Hz, 1H), 1.58 (ddd, *J* = 33.7, 12.6, 3.5 Hz, 2H), 1.45–1.21 (m, 1H), 1.17–0.98 ppm (m, 1H); ^{13}C NMR (75 MHz, $CDCl_3$): δ = 169.8, 152.2, 149.4, 146.7, 144.1, 142.7, 141.2, 140.1, 131.2, 129.3, 125.3, 124.25, 122.8, 121.7, 120.9, 119.5, 118.2, 117.7, 113.7, 112.9, 111.1, 93.0, 70.8, 70.5, 70.4, 70.3, 70.3, 70.2, 69.4, 63.1, 62.8, 59.4, 55.8, 55.3, 53.2, 51.3, 50.3, 50.2, 47.2, 43.4, 42.8, 42.7, 35.3, 28.7, 24.1, 20.0 ppm; HRMS (ESI) *m/z*: calculated for $C_{49}H_{67}N_7O_{10}$ $[M+2H]^{2+}$ 456.7469, found 456.7434.

***N*-((4*R*,4a*R*,7*R*,7a*R*,12b*S*)-9-hydroxy-3-methyl-2,3,4,4a,5,6,7,7a-octahydro-1*H*-4,12-methanobenzofuro[3,2-*e*]isoquinolin-7-yl)-17-(4-((2-methoxy-4-((4-(2-methoxyphenyl)piperazin-1-yl)methyl)phenoxy)methyl)-1*H*-1,2,3-triazol-1-yl)-3,6,9,12,15-pentaoxaheptadecanamide (12e)**: Compound **12e** was subjected to general procedure 2. Off-white solid, 46%. LC–HRMS: t_R = 5.30 min (10–100% MeCN, 15 min run), 88.20%; HRMS (ESI) *m/z*: calculated for $C_{51}H_{71}N_7O_{11}$ $[M+2H]^{2+}$ 478.7600, found 478.7562.

***N*-((4*R*,4a*R*,7*R*,7a*R*,12b*S*)-9-hydroxy-3-methyl-2,3,4,4a,5,6,7,7a-octahydro-1*H*-4,12-methanobenzofuro[3,2-*e*]isoquinolin-7-yl)-20-(4-((2-methoxy-4-((4-(2-methoxyphenyl)piperazin-1-yl)methyl)phenoxy)methyl)-1*H*-1,2,3-triazol-1-yl)-3,6,9,12,15,18-hexaoxaicosanamide (12f)**: Compound **12f** was subjected to general procedure 2. Off-white solid, 40%. LC–HRMS: t_R = 5.37 min (10–100% MeCN, 15 min run), 92.86%. ^{1}H NMR (300 MHz, $CDCl_3$): δ = 7.84 (s, 1H), 7.22 (d, *J* = 9.7 Hz, 1H), 7.02–6.88 (m, 4H), 6.82 (t, *J* = 8.0 Hz, 2H), 6.66 (d, *J* = 8.0 Hz, 1H), 6.55 (d, *J* = 8.1 Hz, 1H), 5.26 (s, 2H), 4.71 (s, 0H), 4.52 (t, *J* = 5.1 Hz, 2H), 4.43 (dd, *J* = 8.0, 3.6 Hz, 1H), 3.92 (s, 2H), 3.85 (d, *J* = 4.3 Hz, 5H), 3.81 (d, *J* = 3.0 Hz, 3H), 3.77–3.45 (m, 29H), 3.19–2.98 (m, 6H), 2.98–2.92 (m, 1H), 2.65 (t, *J* = 4.8 Hz, 4H), 2.51 (dd, *J* = 11.9, 4.4 Hz, 1H), 2.38 (s, 3H), 2.18 (dt, *J* = 15.9, 5.0 Hz, 2H), 1.82 (dt, *J* = 11.6, 5.3 Hz, 2H), 1.71–1.47 (m, 2H), 1.44–1.23 (m, 1H), 1.15–0.99 ppm (m, 1H); ^{13}C NMR (75 MHz, $CDCl_3$): δ = 169.9, 152.2, 149.4, 146.8, 144.1, 142.7, 141.3, 140.2, 131.3 (d, *J* = 4.5 Hz), 129.3, 125.3, 124.2, 122.8, 121.6, 120.9, 119.4, 118.2, 117.5, 113.7, 112.8, 111.1, 93.1, 70.8, 70.5, 70.4, 70.3, 70.2, 69.4, 63.1, 62.8, 59.4, 55.8, 55.3, 53.2, 51.8, 50.3 (d, *J* = 14.4 Hz), 47.2, 43.4, 42.8 (d, *J* = 8.3 Hz), 35.3, 28.7, 24.2, 20.1 ppm; HRMS (ESI) *m/z*: calculated for $C_{53}H_{75}N_7O_{12}$ $[M+2H]^{2+}$ 500.7731, found 500.7742.

***N*-((4*R*,4a*S*,7*R*,7a*R*,12b*S*)-3-(cyclopropylmethyl)-4a,9-dihydroxy-2,3,4,4a,5,6,7,7a-octahydro-1*H*-4,12-methanobenzofuro[3,2-*e*]isoquinolin-7-yl)-14-(4-(3-((4-(2-((5-hydroxy-1,2,3,4-tetrahydronaphthalen-2-yl)(propyl)amino)ethyl)phenyl)amino)-3-oxopropyl)-1*H*-1,2,3-triazol-1-yl)-3,6,9,12-tetraoxatetradecanamide (13a)**: Compound **13a** was subjected to general procedure 2. Off-white solid, 60%. LC–HRMS: t_R = 5.43 min (10–100% MeCN, 15 min run), 99.45%. ^{1}H NMR (300 MHz, $CDCl_3$): δ = 7.40 (d, *J* = 8.2 Hz, 2H), 7.22 (d, *J* = 8.9 Hz, 1H), 7.08 (d, *J* = 8.4 Hz, 2H), 6.94 (t, *J* = 7.8 Hz, 1H), 6.72 (d, *J* = 8.1 Hz, 1H), 6.62 (d, *J* = 7.9 Hz, 2H), 6.53 (d, *J* = 8.2 Hz, 1H), 4.47 (t, *J* = 5.1 Hz, 2H), 4.41 (d, *J* = 7.5 Hz, 1H), 3.92 (s, 2H), 3.83 (t, *J* = 5.2 Hz, 2H), 3.64–3.56 (m, 14H), 3.07 (dt, *J* = 15.4, 6.3 Hz, 3H), 2.99–2.85 (m, 2H), 2.76 (dt, *J* = 14.2, 7.4 Hz, 6H), 2.56 (dt, *J* = 17.0, 7.8 Hz, 4H), 2.35 (d, *J* = 6.5 Hz, 2H), 2.20–1.99 (m, 3H), 1.85 (q, *J* = 12.8 Hz, 1H), 1.71–1.36 (m, 6H), 1.25 (s, 1H), 0.89 (t, *J* = 7.3 Hz, 3H), 0.56–0.48 (m, 2H), 0.11 ppm (q, *J* = 5.0 Hz, 2H); ^{13}C NMR (75 MHz, $CDCl_3$): δ = 170.6, 170.1, 153.8, 146.2, 142.5, 140.3, 137.9, 136.2 (d, *J* = 9.1 Hz), 130.3, 129.1, 126.3, 124.0, 123.1, 122.9, 121.3, 119.9, 119.1, 118.0, 112.1, 92.6, 77.2, 74.6, 70.8, 70.5, 70.4, 70.4, 70.3, 70.3, 70.1, 69.4, 62.3, 59.1, 56.8, 53.4, 52.7 (d, *J* = 18.9 Hz), 51.0, 50.2, 47.6, 44.1, 36.5, 34.9, 32.0, 30.6, 30.0, 25.6, 24.5, 23.5, 22.6, 21.7, 21.3, 11.9, 9.4, 3.9, 3.7 ppm; HRMS (ESI) *m/z*: calculated for $C_{56}H_{77}N_7O_{10}$ $[M+2H]^{2+}$ 503.7860, found 503.7833.

***N*-((4*R*,4a*S*,7*R*,7a*R*,12b*S*)-3-(cyclopropylmethyl)-4a,9-dihydroxy-2,3,4,4a,5,6,7,7a-octahydro-1*H*-4,12-methanobenzofuro[3,2-*e*]isoquinolin-7-yl)-17-(4-(3-((4-(2-((5-hydroxy-1,2,3,4-tetrahydronaphthalen-2-yl)(propyl)amino)ethyl)phenyl)amino)-3-oxopropyl)-1*H*-1,2,3-triazol-1-yl)-3,6,9,12,15-pentaoxaheptadecanamide (13b)**: Compound **13b** was subjected to general procedure 2. Off-white solid, 47%. LC–HRMS: t_R = 5.48 min (10–100% MeCN, 15 min run), 95.65%. ^{1}H NMR (300 MHz, $CDCl_3$): δ = 7.59 (s, 1H), 7.40 (d, *J* = 8.4 Hz, 2H), 7.08 (d, *J* = 8.3 Hz, 2H), 6.95 (t, *J* = 7.8 Hz, 1H), 6.72 (d, *J* = 8.1 Hz, 1H), 6.62 (t, *J* = 7.8 Hz, 2H), 6.54 (d, *J* = 8.1 Hz, 1H), 3.92 (s, 2H), 3.81 (t, *J* = 5.0 Hz, 2H), 3.72–3.48 (m, 18H), 3.17–3.02 (m, 3H), 3.02–2.85 (m, 2H), 2.85–2.65 (m, 5H), 2.63–2.49 (m, 4H), 2.35 (d, *J* = 6.5 Hz, 2H), 2.15 (s, 1H), 1.61–1.38 (m, 3H), 0.89 (t, *J* = 7.3 Hz, 3H), 0.55–0.47 (m, 2H), 0.14–0.09 ppm (m, 2H); ^{13}C NMR (75 MHz, $CDCl_3$): δ = 170.6, 170.0, 153.6, 146.2, 142.5, 140.2, 138.2, 136.5, 136.1, 130.9, 129.0, 126.2, 124.1, 123.1, 122.8, 121.4, 119.8, 119.0, 118.0, 112.0, 92.7, 77.2, 70.8, 70.5, 70.5, 70.4, 70.3, 70.3, 70.1, 69.4, 62.3, 59.1, 56.6, 52.8, 52.5, 51.0, 50.2, 47.7, 44.0, 36.5, 35.2, 32.1, 30.6, 30.0, 25.7, 24.4, 23.5, 22.6, 21.9, 21.3, 11.9, 9.4, 3.9, 3.7 ppm; HRMS (ESI) *m/z*: calculated for $C_{58}H_{81}N_7O_{11}$ $[M+2H]^{2+}$ 525.7991, found 525.8002.

***N*-((4*R*,4a*S*,7*R*,7a*R*,12b*S*)-3-(cyclopropylmethyl)-4a,9-dihydroxy-2,3,4,4a,5,6,7,7a-octahydro-1*H*-4,12-methanobenzofuro[3,2-*e*]isoquinolin-7-yl)-20-(4-(3-((4-(2-((5-hydroxy-1,2,3,4-tetrahydronaphthalen-2-yl)(propyl)amino)ethyl)phenyl)amino)-3-oxopropyl)-1*H*-1,2,3-triazol-1-yl)-3,6,9,12,15,18-hexaoxaicosanamide (13c)**: Compound **13c** was subjected to general procedure 2. Off-white solid, 43%. LC–HRMS: t_R = 5.53 min (10–100% MeCN, 15 min run), 98.35%; HRMS (ESI) *m/z*: calculated for $C_{60}H_{85}N_7O_{12}$ $[M+2H]^{2+}$ 547.8122, found 547.8098.

14-(4-(3-((4-(2-((5-hydroxy-1,2,3,4-tetrahydronaphthalen-2-yl)(propyl)amino)ethyl)phenyl)amino)-3-oxopropyl)-1*H*-1,2,3-triazol-1-yl)-*N*-((4*R*,4a*R*,7*R*,7a*R*,12b*S*)-9-hydroxy-3-methyl-2,3,4,4a,5,6,7,7a-octahydro-1*H*-4,12-methanobenzofuro[3,2-*e*]isoquinolin-7-yl)-3,6,9,12-tetraoxatetradecanamide (13d): Compound **13d** was subjected to general procedure 2. Off-white solid, 52%. LC–HRMS: t_R = 5.26 min (10–100% MeCN, 15 min run), 98.63%. ^{1}H NMR (300 MHz, $CDCl_3$): δ = 8.23 (s, 1H), 7.59 (s, 1H), 7.39 (d, *J* = 8.3 Hz, 2H), 7.09 (d, *J* = 8.1 Hz, 2H), 6.96 (t, *J* = 7.7 Hz,

1H), 6.72 (d, J=8.1 Hz, 1H), 6.64 (d, J=7.6 Hz, 1H), 6.58 (dd, J=8.0, 4.2 Hz, 2H), 4.47 (t, J=5.0 Hz, 2H), 4.37 (d, J=7.9 Hz, 1H), 3.92 (s, 2H), 3.82 (t, J=5.0 Hz, 2H), 3.69–3.50 (m, 14H), 3.11 (d, J=6.9 Hz, 3H), 2.98–2.85 (m, 3H), 2.83–2.66 (m, 6H), 2.55 (dd, J=8.6, 6.5 Hz, 3H), 2.41 (s, 3H), 2.19 (d, J=12.6 Hz, 2H), 2.02 (d, J=12.6 Hz, 1H), 1.81 (td, J=12.2, 11.3, 7.1 Hz, 2H), 1.69–1.57 (m, 1H), 1.50 (q, J=7.1 Hz, 3H), 1.25 (s, 3H), 0.89 ppm (t, J=7.3 Hz, 3H); ^{13}C NMR (75 MHz, $CDCl_3$): δ=170.6, 169.9, 146.2, 153.8, 142.8, 140.2, 136.6, 136.0, 129.1, 126.3, 123.2, 122.8, 121.3, 119.8, 119.5, 117.8, 112.0, 93.0, 70.7, 70.5, 70.4, 70.4, 70.2, 70.2, 69.4, 59.5, 56.7, 53.4, 51.6, 50.1, 47.2, 43.3, 42.5, 36.6, 35.2, 32.1, 29.6, 28.7, 25.7, 24.0, 23.5, 21.9, 21.4, 20.1, 11.9 ppm; HRMS (ESI) m/z: calculated for $C_{53}H_{73}N_7O_9$ $[M+2H]^{2+}$ 475.7729, found 475.7702.

17-(4-(3-((4-(2-((5-hydroxy-1,2,3,4-tetrahydronaphthalen-2-yl)(propyl)amino)ethyl)phenyl)amino)-3-oxopropyl)-1*H*-1,2,3-triazol-1-yl)-*N*-((4*R*,4a*R*,7*R*,7a*R*,12b*S*)-9-hydroxy-3-methyl-2,3,4,4a,5,6,7,7a-octahydro-1*H*-4,12-methanobenzofuro[3,2-*e*]isoquinolin-7-yl)-3,6,9,12,15-pentaoxaheptadecanamide (13 e): Compound **13 e** was subjected to general procedure 2. Off-white solid, 48%. LC–HRMS: t_R=5.33 min (10–100% MeCN, 15 min run), 95.43%; HRMS (ESI) m/z: calculated for $C_{55}H_{77}N_7O_{10}$ $[M+2H]^{2+}$ 497.7860, found 497.7826.

20-(4-(3-((4-(2-((5-hydroxy-1,2,3,4-tetrahydronaphthalen-2-yl)(propyl)amino)ethyl)phenyl)amino)-3-oxopropyl)-1*H*-1,2,3-triazol-1-yl)-*N*-((4*R*,4a*R*,7*R*,7a*R*,12b*S*)-9-hydroxy-3-methyl-2,3,4,4a,5,6,7,7a-octahydro-1*H*-4,12-methanobenzofuro[3,2-*e*]isoquinolin-7-yl)-3,6,9,12,15,18-hexaoxaicosanamide (13 f): Compound **13 f** was subjected to general procedure 2. Off-white solid, 44%. LC–HRMS: t_R=5.37 min (10–100% MeCN, 15 min run), 97.02%. ^{1}H NMR (300 MHz, $CDCl_3$): δ=8.48 (d, J=7.4 Hz, 1H), 7.59 (s, 1H), 7.40 (d, J=7.9 Hz, 2H), 7.07 (d, J=8.0 Hz, 2H), 6.93 (t, J=7.7 Hz, 1H), 6.69 (d, J=8.1 Hz, 1H), 6.58 (q, J=8.6 Hz, 3H), 5.29 (s, 1H), 4.52–4.35 (m, 3H), 3.90 (s, 2H), 3.79 (t, J=5.0 Hz, 2H), 3.71–3.42 (m, 22H), 3.10 (t, J=6.7 Hz, 3H), 2.94 (td, J=13.9, 13.5, 7.0 Hz, 2H), 2.83–2.62 (m, 6H), 2.62–2.44 (m, 4H), 2.38 (s, 3H), 2.18 (dt, J=12.5, 4.2 Hz, 2H), 2.02 (d, J=11.2 Hz, 1H), 1.80 (t, J=11.9 Hz, 1H), 1.69–1.40 (m, 4H), 1.27 (d, J=12.9 Hz, 1H), 1.03 (t, J=12.9 Hz, 1H), 0.88 ppm (t, J=7.3 Hz, 3H); ^{13}C NMR (75 MHz, $CDCl_3$): δ=170.6, 170.1, 154.1, 146.3, 142.8, 140.3, 138.1, 136.4, 136.2, 129.2, 129.0, 126.2, 125.0, 123.4, 122.9, 121.0, 119.8, 119.4, 117.7, 111.9, 92.9, 70.7, 70.5, 70.4, 70.3, 70.3, 70.2, 69.3, 59.4, 56.7, 52.8, 52.6, 51.6, 50.2, 47.2, 43.3, 42.5 (d, J=11.1 Hz), 36.4, 35.1 (d, J=8.9 Hz), 32.2, 28.7, 25.8, 24.1, 23.7, 22.0, 21.3, 20.1 ppm; HRMS (ESI) m/z: calculated for $C_{57}H_{81}N_7O_{11}$ $[M+2H]^{2+}$ 519.7991, found 519.7953.

Plasmids and receptor fusion constructs

The plasmids HA $D_{4.2}$ and HA D_2 were described previously.[39] The NanoBiT constructs (NB MCS1) and (NB MCS2) were procured from Promega. These plasmids encode for the split fragments of Nanoluciferase: LargeBiT (LgBiT) and SmallBiT (SmBiT). The human μOR was PCR amplified and SmBiT was cloned at the C-terminus of the receptor. A flexible linker (GSSGGGGSGGGGSSG) is present in between μOR and SmBiT. To clone μOR-SmBiT, specific primers were generated with a *Hind*III restriction site at the 5′ terminus and a *Xho*I site at the 3′ terminus of the μOR coding sequence by removing the stop codon. PCR was performed with 20 ng of plasmid with *Pfu* DNA Polymerase (2.5 U μL^{-1}, Thermo Fisher Scientific) according to the manufacturer's protocol. The reactions were performed in a Mastercycler Nexus Thermal Cycler (Eppendorf, Hamburg, Germany) and then purified using QIAquick Gel Extraction Kit (QIAGEN, Germany). The resultant amplicon and the vector (NB MCS2) were digested with *Hind*III and *Xho*I for 3 h at 37 °C. The digested PCR product was cleaned using "High Pure PCR Product Purification Kit" (Roche, Germany) and then ligated into the corresponding digested NB MCS2. After transformation of the ligated product into competent MC 1061 "*E. coli*" strain, the ampicillin resistant clones were screened by performing PCR with primers against μOR. Furthermore, a digestion was performed with *Hind*III and *Xba*I, which are the restriction sites flanking μOR-SmBiT. The constructs were verified by sequencing. LgBiT-β-arrestin 2 has been previously described.[32]

Cell culture and transfection

Human embryonic kidney (HEK) 293T cells were cultured in Dulbecco's modified Eagle's medium (DMEM; Invitrogen), supplemented with 10% fetal bovine serum, penicillin (100 U mL^{-1}), and streptomycin (100 μg mL^{-1}) in a controlled environment (37 °C, 98% humidity, 5% CO_2). For ligand binding experiments and β-arrestin 2 recruitment assay, HEK293T cells were transiently transfected using the Polyethylenimine (PEI) method as described before.[30] A total amount of 10 μg of DNA was used for transfection of cells in one 10 cm dish. HEK293S cells stably expressing HA $D_{4.2}R$[30] were grown in DMEM/F12 (Gibco, Invitrogen) supplemented with 10% fetal bovine serum, penicillin (100 U mL^{-1}), streptomycin (100 μg mL^{-1}), and 0.5 mg mL^{-1} G418 (Geneticin, Gibco) in a controlled environment (37 °C, 98% humidity, 5% CO_2).

Membrane preparation and protein determination

Membrane suspensions from HEK293T cells transiently transfected with the receptors of interest were prepared as described previously.[27,28] Cells were disrupted with a Polytron homogenizer for two 10 s periods in 10 volumes of ice-cold Tris·HCl buffer (50 mM, pH 7.4). Membranes were obtained by centrifugation at 16500 g for 20 min at 4 °C, and the pellet was resuspended and centrifuged under the same conditions. The resulting pellet was stored at −80 °C and was washed once more as described above and resuspended in Tris·HCl buffer (50 mM, pH 7.4) for immediate use. Protein was quantified by the BCA method using bovine serum albumin dilutions as the standard.

[^{3}H]Spiperone binding

Saturation binding assay for [^{3}H]spiperone was performed as previously.[27,28] For competition binding assays, membranes (20 μg) were incubated in binding buffer (50 mM Tris·HCl containing 5 mM KCl, 1 mM EDTA, 1.5 mM $CaCl_2$ and 4 mM $MgCl_2$, pH 7.4) with 0.2 nM [^{3}H] spiperone (specific activity=76 Ci mmol^{-1}, PerkinElmer, USA) in the absence or presence of 11 different concentrations (0.1 nM–10 μM) of unlabeled ligands for 1 h at 22 °C. Nonspecific binding was determined in the presence of 1 μM haloperidol. Incubation was terminated by rapid filtration through GF/C glass-fiber filters (Whatman Schleicher and Schuell, Keene, NH) embedded in 0.1% polyethylenimine and mounted on a Brandel cell harvester. Filters were washed three times with cold 50 mM Tris·HCl, pH 7.4 buffer and transferred to vials containing 3 mL of scintillation cocktail to soak the filter overnight. The radioactivity counts were measured with a Tri-Carb 2800TR liquid scintillation analyzer (PerkinElmer).

[^{3}H]Raclopride binding

[^{3}H]raclopride saturation binding assay was performed as described before.[40] Briefly, a suspension of whole cells (corresponding a total protein amount of 20 μg) were incubated with different concentrations (0–20 nM) of [^{3}H]raclopride in 50 mM Tris·HCl, pH 7.4 buffer (containing 5 mM KCl, 100 mM NaCl, 1.5 mM $CaCl_2$, 4 mM $MgCl_2$ and 1 mM EDTA) at 37 °C for 1 h. For competitive binding experiments, 2.0 nM [^{3}H]raclopride (specific activity = 73.8 Ci mmol^{-1}, PerkinElmer, USA) was incubated with 20 μg of whole cells in the absence or presence of varying concentrations (0.1 nM^{-1}0 μM) of unlabeled ligands at 37 °C for 1 h. Nonspecific binding was determined in the presence of 1 μM haloperidol. Free and cell-bound ligand were separated by rapid filtration through GF/C glass-fiber filters (Whatman Schleicher and Schuell, Keene, NH) embedded in 0.1% polyethylenimine and mounted on a Brandel cell harvester. Filtration and measuring were as described above.

[^{3}H]Diprenorphine binding

[^{3}H]diprenorphine saturation binding assay was adapted from a published protocol.[41] Membranes (10 μg) were incubated with different concentrations (0–6 nM) of [^{3}H]diprenorphine in 50 mM Tris·HCl, pH 7.4 buffer at 25 °C for 1 h. For competitive binding experiments, 0.5 nM [^{3}H]diprenorphine (specific activity = 25.8 Ci mmol^{-1}, PerkinElmer, USA) was incubated with 10 μg of membranes in the absence or presence of varying concentrations (0.1 nM^{-1}0 μM) of unlabeled ligands at 25 °C for 1 h. Nonspecific binding was determined in the presence of 10 μM naloxone. Filtration and measuring were as described above.

Data analysis: Results are expressed as means ± SEM for at least three experiments, each performed in duplicate. Statistical analysis and curve fits of dose-response curves were performed using GraphPad Prism 7. K_i values were calculated by using the Cheng–Prusoff equation.[42]

MAPK phosphorylation

HEK293S cells stably expressing HA $D_{4.2}$R were seeded in 6-well plates at 400000 cells per well. When the cells were 70% confluent, cells were starved overnight with serum free medium. The ligands (1 nM–10 μM) were added sequentially to the cells at the concentrations indicated in the legend for 5 min. To stop the reaction, medium was aspirated, the cells were placed on ice and washed with ice-cold PBS. RIPA buffer [150 mM NaCl; 50 mM Tris/HCl pH 7.5; 1% NP-40; 0.1% SDS; and 0.5% deoxycholic acid sodium salt (Acros Organics: 218591000). protease inhibitors: aprotinin (2.5 μg mL^{-1}, Sigma–Aldrich: A6279), pefablock (1 mM, Sigma–Aldrich: 76307), leupeptin (10 μg mL^{-1}, Acros Organics: 328350050), and phosphatase inhibitor β-glycerol phosphate disodium salt pentahydrate (10 mM, Fluka BioChemika: 50020) was used to prepare the cell lysate for western blotting according to the protocol described before.[43] After western blotting, the membrane was incubated with blocking buffer (LI-COR Biosciences) for 1 h at RT. Then, primary antibody rabbit polyclonal phospho-p44/42 MAPK (1/2000) (Cell Signaling, cat. no. 9101L) or mouse monoclonal p44/42 MAPK (1/2000) (clone L34F12; Cell Signaling, cat. no. 4696S) was added to develop the blot overnight at 4 °C. Next, the blot was washed with washing buffer (PBS + 0.05% Tween 20 from Sigma–Aldrich) for three times and then secondary antibodies goat anti-rabbit IRDye680 LT (1/10000) (cat. no. 926-68021, LI-COR Biosciences) or goat anti-mouse IRDye800 (1/10000) (cat. no.926-32210, LI-COR Biosciences) were added for 1 h at RT in the dark. The blot was washed three times with washing buffer and the fluorescent signal was detected with the Odyssey Infrared Imaging system. In the analysis, the phospho-p44/42 MAPK signal is normalized against the total p44/42 MAPK signal after quantification by ImageJ.

β-Arrestin 2 recruitment

HEK293T cells were seeded in 10-cm dishes with 2.5×10^6 cells/dish and transiently transfected with pμOR-SmBiT (4 μg), pLgBiT-β-arrestin 2 (1 μg), pGRK2 (1 μg) and pcDNA3 (4 μg) per 10-cm dish. Forty-eight hours after transfection, the cells were washed with warm PBS, a cell suspension was prepared with warm HBSS and proteins were estimated by the bicinchoninic acid method (BCA, Thermo Scientific) using bovine serum albumin dilutions as the standard. The cell suspension was added to a 96-well plate (100 μL cell suspension in each well corresponding to 800 ng protein). The Nano-Glo Live Cell reagent, a nonlytic detection reagent containing the cell permeable furimazine substrate, was prepared by diluting the Nano-Glo Live Cell substrate 20× using Nano-Glo LCS Dilution buffer, and 25 μL was added to each well. Subsequently, the plate was placed in the luminodetecter (CLARIOstar) for measurement. Luminescence was monitored during the equilibration period until the signal was stabilized before adding the agonists of μOR (0.1 nM^{-1}0 μM, 14 μL). After adding the test compounds, luminescence was continuously detected for 20–22 cycles. Solvent controls were run in all experiments.

Acknowledgements

This project is financially supported by the China Scholarship Council and Fonds voor Wetenschappelijk Onderzoek – Vlaanderen (FWO; G021715N).

Conflict of interest

The authors declare no conflict of interest.

Keywords: bivalent ligands · dopamine D_2-like receptors · ligand binding · signal transduction · μ-opioid receptors

[1] L. F. Agnati, K. Fuxe, I. Zini, P. Lenzi, T. Hökfelt, *Med. Biol.* **1980**, *58*, 182.
[2] K. Fuxe, L. F. Agnati, F. Benfenati, M. Cimmino, S. Algeri, T. Hökfelt, V. Mutt, *Acta Physiol. Scand.* **1981**, *113*, 567.
[3] J. H. White, A. Wise, M. J. Main, A. Green, N. J. Fraser, G. H. Disney, A. A. Barnes, P. Emson, S. M. Foord, F. H. Marshall, *Nature* **1998**, *396*, 679.
[4] K. Fuxe, D. Marcellino, A. S. Woods, L. Giuseppina, T. Antonelli, L. Ferraro, S. Tanganelli, L. F. Agnati, *J. Neural Transm.* **2009**, *116*, 923.
[5] G. Milligan, *Curr. Opin. Pharmacol.* **2010**, *10*, 23.
[6] D. J. Daniels, N. R. Lenard, C. L. Etienne, P. Y. Law, S. C. Roerig, P. S. Portoghese, *Proc. Natl. Acad. Sci. USA* **2005**, *102*, 19208.
[7] D. J. Daniels, A. Kulkarni, Z. Xie, R. G. Bhushan, P. S. Portoghese, *J. Med. Chem.* **2005**, *48*, 1713.
[8] N. R. Lenard, D. J. Daniels, P. S. Portoghese, S. C. Roerig, *Eur. J. Pharmacol.* **2007**, *566*, 75.
[9] G. Milligan, M. Bouvier, *FEBS J.* **2005**, *272*, 2914.
[10] A. S. Yekkirala, M. M. Lunzer, C. R. McCurdy, M. D. Powers, A. E. Kalyuzhny, S. C. Roerig, P. S. Portoghese, *Proc. Natl. Acad. Sci. USA* **2011**, *108*, 5098.
[11] A. Soriano, R. Ventura, A. Molero, R. Hoen, V. Casadó, A. Cortés, F. Fanelli, F. Albericio, C. Lluís, R. Franco, M. Royo, *J. Med. Chem.* **2009**, *52*, 5590.

[12] K. A. Jacobson, R. Xie, L. Young, L. Chang, B. T. Liang, *J. Biol. Chem.* **2000**, *275*, 30272.
[13] P. S. Portoghese, *J. Med. Chem.* **2001**, *44*, 2259.
[14] L. M. Ambrose, E. M. Unterwald, E. J. Van Bockstaele, *Anat. Rec. Part A* **2004**, *279*, 583.
[15] A. Rivera, B. Cuéllar, F. J. Girón, D. K. Grandy, A. de la Calle, R. Moratalla, *J. Neurochem.* **2002**, *80*, 219.
[16] B. Gago, D. Suárez-Boomgaard, K. Fuxe, S. Brené, M. D. Reina-Sánchez, L. M. Rodríguez-Pérez, L. F. Agnati, A. de la Calle, A. Rivera, *Brain Res.* **2011**, *1407*, 47.
[17] B. Gago, K. Fuxe, L. Agnati, A. Peñafiel, A. De La Calle, A. Rivera, *J. Comp. Neurol.* **2007**, *502*, 358.
[18] N. Hagelberg, J. K. Kajander, K. Någren, S. Hinkka, J. Hietala, H. Scheinin, *Synapse* **2002**, *45*, 25.
[19] Y. Park, I. K. Ho, L. W. Fan, H. H. Loh, K. H. Ko, *Brain Res.* **2001**, *894*, 311.
[20] J. Kühhorn, H. Hübner, P. Gmeiner, *J. Med. Chem.* **2011**, *54*, 4896.
[21] S. Gogoi, S. Biswas, G. Modi, T. Antonio, M. E. Reith, A. K. Dutta, *ACS Med. Chem. Lett.* **2012**, *3*, 991.
[22] G. Cami-Kobeci, A. P. Neal, F. A. Bradbury, L. C. Purington, M. D. Aceto, L. S. Harris, J. W. Lewis, J. R. Traynor, S. M. Husbands, *J. Med. Chem.* **2009**, *52*, 1546.
[23] S. Ghirmai, M. R. Azar, W. E. Polgar, I. Berzetei-Gurske, J. R. Cashman, *J. Med. Chem.* **2008**, *51*, 1913.
[24] Z. Wan, Y. Li, S. Bo, M. Gao, X. Wang, K. Zeng, X. Tao, X. Li, Z. Yang, Z.-X. Jiang, *Org. Biomol. Chem.* **2016**, *14*, 7912.
[25] A. M. Bondia, N. Larcher, L. Garrelly, J. C. Rossi, R. Pascal, *Tetrahedron Lett.* **2010**, *51*, 3330.
[26] P. I. Abronina, A. I. Zinin, A. V. Orlova, S. L. Sedinkin, L. O. Kononov, *Tetrahedron Lett.* **2013**, *54*, 4533.
[27] J. P. Van Wieringen, M. C. Michel, **2013**, *3*, DOI: https://doi.org/10.21769/BioProtoc.944.
[28] K. Van Craenenbroeck, S. D. Clark, M. J. Cox, J. N. Oak, F. Liu, H. H. Van Tol, *J. Biol. Chem.* **2005**, *280*, 19350.
[29] G. Pearson, F. Robinson, T. B. Gibson, B. E. Xu, M. Karandikar, K. Berman, M. H. Cobb, *Endocr. Rev.* **2001**, *22*, 153.
[30] K. Skieterska, P. Rondou, B. Lintermans, K. Van Craenenbroeck, *PLoS One* **2015**, *10*, e0145654.
[31] A. S. Dixon, M. K. Schwinn, M. P. Hall, K. Zimmerman, P. Otto, T. H. Lubben, B. L. Butler, B. F. Binkowski, T. Machleidt, T. A. Kirkland, M. G. Wood, C. T. Eggers, L. P. Encell, K. V. Wood, *ACS Chem. Biol.* **2016**, *11*, 400.
[32] A. Cannaert, J. Storme, F. Franz, V. Auwärter, C. P. Stove, *Anal. Chem.* **2016**, *88*, 11476.
[33] C. E. Groer, K. Tidgewell, R. A. Moyer, W. W. Harding, R. B. Rothman, T. E. Prisinzano, L. M. Bohn, *Mol. Pharmacol.* **2007**, *71*, 549.
[34] C. E. Groer, C. L. Schmid, A. M. Jaeger, L. M. Bohn, *J. Biol. Chem.* **2011**, *286*, 31731.
[35] J. Zhang, S. S. Ferguson, L. S. Barak, S. R. Bodduluri, S. A. Laporte, P. Y. Law, M. G. Caron, *Proc. Natl. Acad. Sci. USA* **1998**, *95*, 7157.
[36] H. Hübner, T. Schellhorn, M. Gienger, C. Schaab, J. Kaindl, L. Leeb, T. Clark, D. Möller, P. Gmeiner, *Nat. Commun.* **2016**, *7*, 12298.
[37] M. Le Naour, E. Akgün, A. Yekkirala, M. M. Lunzer, M. D. Powers, A. E. Kalyuzhny, P. S. Portoghese, *J. Med. Chem.* **2013**, *56*, 5505.
[38] R. Corriden, L. E. Kilpatrick, B. Kellam, S. J. Briddon, S. J. Hill, *FASEB J.* **2014**, *28*, 4211.
[39] P. Rondou, G. Haegeman, P. Vanhoenacker, K. Van Craenenbroeck, *J. Biol. Chem.* **2008**, *283*, 11083.
[40] B. Kiss, F. Horti, A. Bobok, *Synapse* **2011**, *65*, 467.
[41] D. Wang, X. Sun, W. Sadee, *J. Pharmacol. Exp. Ther.* **2007**, *321*, 544.
[42] Y. Cheng, W. H. Prusoff, *Biochem. Pharmacol.* **1973**, *22*, 3099.
[43] K. Skieterska, J. Duchou, B. Lintermans, K. Van Craenenbroeck, *Methods Cell Biol.* **2013**, *117*, 323.

Manuscript received: December 15, 2017
Accepted manuscript online: February 16, 2018
Version of record online: April 16, 2018